SCATTERING PROPERTIES OF JOINTS IN COMPOSITE PLATES

Giannoula Mitrou[†], Jamil Renno[‡]

Institute of Sound and Vibration Research
University of Southampton, Southampton SO17 1BJ, UK
Email: g.mitrou@soton.ac.uk

ABSTRACT

The aim of this work is to demonstrate how the wave and finite element (WFE) method can be used for the prediction of the scattering of waves in joined flat panels that are homogeneous in two directions but that could be arbitrarily complicated through the thickness. The WFE method is based on analysing the FE model of, typically, a rectangular segment of the plate through its thickness. This FE model can be obtained using standard FE libraries and commercial or in-house packages can be equally exploited with the only restriction being that the nodes and the corresponding degrees of freedom are identically arranged at each edge. The FE model of the segment is post-processed using periodic structure theory to formulate an eigenproblem whose solution includes complete information of the wave characteristics of the plate. For joined panels, the wave behaviour of each panel is obtained using the WFE method and the joint is modelled using standard FE with a matching number of nodes at the interface with each panel. Then, continuity and equilibrium conditions are enforced at the interfaces. Coupling the WFE and FE models can be utilised to deduce the scattering of waves through the joint. Furthermore, the flow of power can be investigated at different frequencies and in various incidence directions.

[†]Corresponding, presenting author.

[‡]Currently at Plant Integrity Department, Doosan Babcock, Porterfield Road, Renfrew PA4 8HR, email: jamil.renno@doosan.com

1 INTRODUCTION

The prediction of disturbance transmission, energy transport and acoustic radiation from composite structures is of great importance for many applications. Composite plates are generally used for buildings, bridges, vehicles and many other structures. A typical composite plate can comprise many layers of different properties and orientations. Details about the mechanics of laminated composite plates can be found in [1]. Developing analytical models that describe the dynamic behaviour of such plates can be a very difficult task. Although layer-wise theories can be used, the resulting governing equations can be cumbersome and the dispersion equations can be of very high order or transcendental. As an alternative, numerical techniques such as the finite element (FE) method are often used; however, FE models become impractically large at high frequencies.

In recent years, the wave and finite element (WFE) method has been proposed and developed to model the wave behaviour of complicated media that is homogeneous in one or two directions. One of the early works on this method can be found in [4]. This method has also been further applied to study thin plates [5, 6], laminated plates [7], fluid-filled pipes [8, 9], cylindrical structures [10, 11] and to predict the free [7] and forced [12] response.

For simple cases, the scattering properties of joints can be obtained by analytical solutions, see [2, 3]. Whereas, in case of more complicated structures, such as plate/beam junctions [13], bolted joints [14] and curved beams [15], wave approaches can been used to find the reflection and transmission coefficients. The hybrid FE/WFE approach for the computation of the scattering properties of joints in structures comprised of waveguides is introduced in [16].

The aim of this paper is to calculate the scattering properties of the joint in case of two-dimensional structures by using the hybrid FE/WFE method. In section 2 the WFE method in plates is presented. The scattering properties of waves in plates is discussed in section 3. Section 4 includes some numerical results about the dispersion curves and the power flow at different frequencies and incidence directions. Conclusions are drawn in section 5.

2 WFE METHOD IN TWO-DIMENSIONAL STRUCTURES

In this section, the WFE method for two-dimensional structures is briefly reviewed [5]. Time-harmonic motion of the form $\exp[\imath(\omega t - k_x x - k_y y)]$ is assumed where $k_x = k\cos\theta$ and $k_y = k\sin\theta$ are the components of the wavenumber k in the x and y directions, i.e., the wave is travelling in the θ direction. The wavenumbers might be: real for propagating waves in the absence of damping, pure imaginary for evanescent waves or complex for oscillating, decaying waves. Consider a solid which is homogeneous in both the x and y directions, but whose

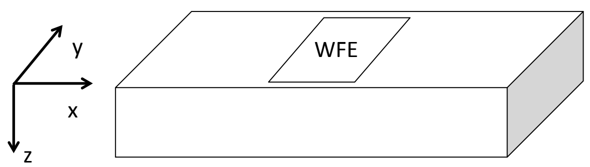

Figure 1: Segment for the WFE modelling of the plate.

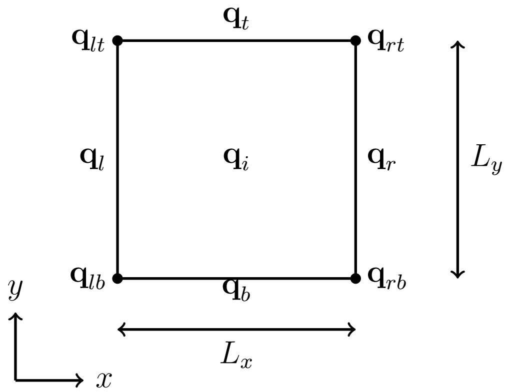

Figure 2: Rectangular segment.

properties may vary arbitrarily through its thickness in the z-direction, see Figure 1. The WFE method starts with a FE model of a small rectangular segment in the (x,y) plane of the plate with sides of lengths L_x and L_y as in Figure 2. This segment is meshed through the thickness using any number of elements: the only condition is that the nodes and degrees of freedom (dofs) are identically arranged on the opposite sides of the segment. Consequently, in case of laminated panels any number of layers and any stacking sequence can be considered.

The vector of dofs $\mathbf{q}$ is partitioned as

$$\mathbf{q} = [\mathbf{q}_{lb}^T \quad \mathbf{q}_{rb}^T \quad \mathbf{q}_{lt}^T \quad \mathbf{q}_{rt}^T \quad \mathbf{q}_{b}^T \quad \mathbf{q}_{r}^T \quad \mathbf{q}_{t}^T \quad \mathbf{q}_{l}^T \quad \mathbf{q}_{i}^T]^T \ .$$

The vector of nodal forces $\mathbf{f}$ is partitioned in a similar manner. For time harmonic motion at frequency ω and in absence of external forces, the governing equation of the segment is $\mathbf{Dq} = \mathbf{f}$, where $\mathbf{D} = (\mathbf{K} + \imath\omega\mathbf{C} - \omega^2\mathbf{M})$ is the stiffness matrix and $\mathbf{K}$, $\mathbf{C}$, and $\mathbf{M}$ are the stiffness, viscous damping and mass matrices, respectively. Under the free passage of a wave whose component in the y direction is k_y, a transformation matrix $\mathbf{R}$ relates the full vector of dofs to a reduced set of dofs as

$$\mathbf{q} = \mathbf{R}\mathbf{q}_{red} \ , \quad \text{where} \quad \mathbf{q}_{red} = \left\{ \begin{array}{c} \mathbf{q}_{lb} \\ \mathbf{q}_{l} \\ \hline \mathbf{q}_{rb} \\ \mathbf{q}_{r} \\ \hline \mathbf{q}_{b} \\ \mathbf{q}_{i} \end{array} \right\} = \left\{ \begin{array}{c} \mathbf{q}_L \\ \mathbf{q}_R \\ \mathbf{q}_O \end{array} \right\} \ .$$

The transformation matrix $\mathbf{R}$ depends on the propagation constant $\lambda_y = \exp(-\imath k_y L_y)$ and is given as

$$\mathbf{R} \cong \mathbf{R}(\lambda_y) = \begin{bmatrix} \mathbf{I} & \mathbf{0} & \mathbf{0} & \mathbf{0} & \mathbf{0} & \mathbf{0} \\ \mathbf{0} & \mathbf{0} & \mathbf{I} & \mathbf{0} & \mathbf{0} & \mathbf{0} \\ \lambda_y\mathbf{I} & \mathbf{0} & \mathbf{0} & \mathbf{0} & \mathbf{0} & \mathbf{0} \\ \mathbf{0} & \mathbf{0} & \lambda_y\mathbf{I} & \mathbf{0} & \mathbf{0} & \mathbf{0} \\ \mathbf{0} & \mathbf{0} & \mathbf{0} & \mathbf{0} & \mathbf{I} & \mathbf{0} \\ \mathbf{0} & \mathbf{0} & \mathbf{0} & \mathbf{I} & \mathbf{0} & \mathbf{0} \\ \mathbf{0} & \mathbf{0} & \mathbf{0} & \mathbf{0} & \lambda_y\mathbf{I} & \mathbf{0} \\ \mathbf{0} & \mathbf{I} & \mathbf{0} & \mathbf{0} & \mathbf{0} & \mathbf{0} \\ \mathbf{0} & \mathbf{0} & \mathbf{0} & \mathbf{0} & \mathbf{0} & \mathbf{I} \end{bmatrix} \ .$$

Hence, the governing equation can be written in terms of the reduced dofs as

$$\mathbf{R}^H(\mathbf{K} + \imath\omega\mathbf{C} - \omega^2\mathbf{M})\mathbf{R}\mathbf{q}_{red} = \mathbf{f}_{red} \ , \tag{1}$$

where H is the Hermitian matrix operator and

$$\mathbf{f}_{red} := \mathbf{R}^H\mathbf{f} = \left\{ \begin{array}{c} \mathbf{f}_{lb} + \lambda_y^{-1}\mathbf{f}_{lt} \\ \mathbf{f}_{l} \\ \hline \mathbf{f}_{rb} + \lambda_y^{-1}\mathbf{f}_{rt} \\ \mathbf{f}_{r} \\ \hline \mathbf{f}_{b} + \lambda_y^{-1}\mathbf{f}_{t} \\ \mathbf{f}_{i} \end{array} \right\} = \left\{ \begin{array}{c} \mathbf{f}_L \\ \mathbf{f}_R \\ \mathbf{f}_O \end{array} \right\} \ .$$

Since the internal nodal forces are zero, $\mathbf{f}_i = \mathbf{0}$, and due to the equilibrium conditions at the bottom edge of the segment $\mathbf{f}_b + \lambda_y^{-1}\mathbf{f}_t = \mathbf{0}$ then $\mathbf{f}_O = \mathbf{0}$. Thus, Equation 1 can be expressed as $\widetilde{\mathbf{D}}\mathbf{q}_{red} = \mathbf{f}_{red}$, where $\widetilde{\mathbf{D}} = \mathbf{R}^H[\mathbf{K} + \imath\omega\mathbf{C} - \omega^2\mathbf{M}]\mathbf{R}$; this can be rearranged into

$$\begin{bmatrix} \widetilde{\mathbf{D}}_{LL} & \widetilde{\mathbf{D}}_{LR} & \widetilde{\mathbf{D}}_{LO} \\ \widetilde{\mathbf{D}}_{RL} & \widetilde{\mathbf{D}}_{RR} & \widetilde{\mathbf{D}}_{RO} \\ \widetilde{\mathbf{D}}_{OL} & \widetilde{\mathbf{D}}_{OR} & \widetilde{\mathbf{D}}_{OO} \end{bmatrix} \left\{ \begin{array}{c} \mathbf{q}_L \\ \mathbf{q}_R \\ \mathbf{q}_O \end{array} \right\} = \left\{ \begin{array}{c} \mathbf{f}_L \\ \mathbf{f}_R \\ \mathbf{0} \end{array} \right\} \ . \tag{2}$$

The dofs in $\mathbf{q}_O$ can be eliminated, and the following form is obtained

$$\begin{bmatrix} \mathbf{D}_{LL} & \mathbf{D}_{LR} \\ \mathbf{D}_{RL} & \mathbf{D}_{RR} \end{bmatrix} \begin{Bmatrix} \mathbf{q}_L \\ \mathbf{q}_R \end{Bmatrix} = \begin{Bmatrix} \mathbf{f}_L \\ \mathbf{f}_R \end{Bmatrix} . \quad (3)$$

This formulation of the governing equation corresponds to the one-dimensional formulation of the WFE method introduced in [7]. The propagation constant in the x-direction $\lambda_x = \exp(-\imath k_x L_x)$ can be found by stating the periodicity and equilibrium conditions between the left and right edges of the segment

$$\mathbf{q}_R = \lambda_x \mathbf{q}_L \quad \text{and} \quad \lambda_x \mathbf{f}_L + \mathbf{f}_R = \mathbf{0} \quad (4)$$

and by formulating the eigenvalue problem

$$\mathbf{T} \begin{Bmatrix} \mathbf{q}_L \\ \mathbf{f}_L \end{Bmatrix} = \lambda_x \begin{Bmatrix} \mathbf{q}_L \\ \mathbf{f}_L \end{Bmatrix}, \quad \text{where} \quad \mathbf{T} = \begin{bmatrix} -\mathbf{D}_{LR}^{-1}\mathbf{D}_{LL} & \mathbf{D}_{LR}^{-1} \\ -\mathbf{D}_{RL} + \mathbf{D}_{RR}\mathbf{D}_{LR}^{-1}\mathbf{D}_{LL} & -\mathbf{D}_{RR}\mathbf{D}_{LR}^{-1} \end{bmatrix} \quad (5)$$

is the transfer matrix. A number of better-conditioned eigenproblems can be formulated [17]. Regardless of the eigenproblem used, its solution yield the WFE estimate of the wavenumber k_x and the wavemode shapes, which form the wave basis. The eigenvalues and the associated eigenvectors of the transfer matrix occur in pairs $(\lambda_x^+, \boldsymbol{\phi}^+)$ and $(\lambda_x^-, \boldsymbol{\phi}^-)$, which represent a pair of positive-and negative-going waves [17, 18]. From the computed waves, by applying the criterion $|k_x L_x| < 1$, only the propagating waves and the slowly decaying waves are retained at each frequency. Reducing the wave basis will: (a) reduce the size of the model and (b) improve the conditioning of the system [19].

With the positive- and negative-going waves identified and the eigenvectors partitioned to demonstrate the influence of the nodal dofs and forces the vectors **q** and **f** can be written in terms of the wave amplitudes $\mathbf{a}^{\pm}$, i.e.,

$$\mathbf{q} = \mathbf{\Phi}_\mathbf{q}^+ \mathbf{a}^+ + \mathbf{\Phi}_\mathbf{q}^- \mathbf{a}^- \quad , \quad \mathbf{f} = \mathbf{\Phi}_\mathbf{f}^+ \mathbf{a}^+ + \mathbf{\Phi}_\mathbf{f}^- \mathbf{a}^- . \quad (6)$$

These matrices define a transformation between the physical domain, where the motion is described in terms of **q** and **f**, and the wave domain, where the motion is described in terms of waves of amplitudes $\mathbf{a}^{\pm}$ that travel in the positive and negative x-directions, respectively.

The knowledge of the wavemodes can be further used to find the time-averaged power of the waves as

$$\Pi = \frac{1}{2} \mathbf{a}^H \mathbf{P} \mathbf{a} ,$$

where $\mathbf{a} = [(\mathbf{a}^+)^T \; (\mathbf{a}^-)^T]^T$ and **P** is the power matrix that can be expressed as

$$\mathbf{P} = \frac{i\omega}{2} \left\{ \begin{bmatrix} (\mathbf{\Phi}_\mathbf{q}^+)^H \mathbf{\Phi}_\mathbf{f}^+ & (\mathbf{\Phi}_\mathbf{q}^+)^H \mathbf{\Phi}_\mathbf{f}^- \\ (\mathbf{\Phi}_\mathbf{q}^-)^H \mathbf{\Phi}_\mathbf{f}^+ & (\mathbf{\Phi}_\mathbf{q}^-)^H \mathbf{\Phi}_\mathbf{f}^- \end{bmatrix} - \begin{bmatrix} (\mathbf{\Phi}_\mathbf{f}^+)^H \mathbf{\Phi}_\mathbf{q}^+ & (\mathbf{\Phi}_\mathbf{f}^+)^H \mathbf{\Phi}_\mathbf{q}^- \\ (\mathbf{\Phi}_\mathbf{f}^-)^H \mathbf{\Phi}_\mathbf{q}^+ & (\mathbf{\Phi}_\mathbf{f}^-)^H \mathbf{\Phi}_\mathbf{q}^- \end{bmatrix} \right\} . \quad (7)$$

The power matrix is Hermitian and thus the time averaged power Π is always real.

3 REFLECTION AND TRANSMISSION COEFFICIENTS OF JOINTS

Structures can include discontinuities such as boundaries, line junctions or joints of finite dimensions, whose scattering properties are of a great importance for the structural vibration analysis.

Consider a straight line junction between two plates, see Figure 3. Waves in "Plate 1" of amplitudes $\mathbf{a}^+$ are incident on the joint and they give rise to reflected waves of amplitudes

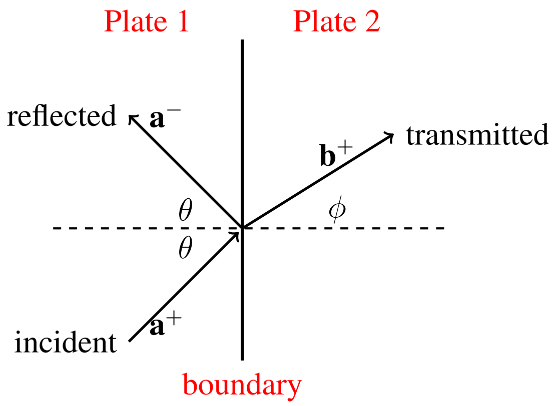

Figure 3: Reflection and transmission on a joint.

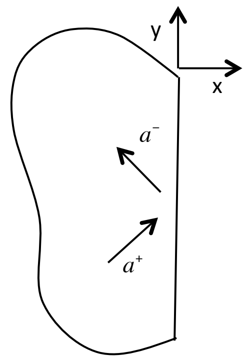

Figure 4: Simply supported plate.

$\mathbf{a}^- = \mathbf{r}_{11}\mathbf{a}^+$ and transmitted waves in "Plate 2" of amplitudes $\mathbf{b}^+ = \mathbf{t}_{12}\mathbf{a}^-$, where $\mathbf{r}_{11}$ and $\mathbf{t}_{12}$ are the matrices of the reflection and transmission coefficients of the joint. These define the scattering matrix $\mathbf{s}$ of the joint, whose partitions relate the amplitudes of the incident and scattered waves.

Denoting by j the wavemodes and by a_j the wave amplitude, from Equation 7, the power flow of the j-th wave is given by $P_{jj}|a_j|^2$. For an incoming wave denoted by j and by using the indices i and k for reflected and transmitted waves, respectively, the reflection and transmission coefficients are computed by

$$\mathcal{R} = [R_{ij}] = \left[|r_{ij}|^2 \frac{P_{ii}}{P_{jj}} \right] \quad \text{and} \quad \mathcal{T} = [T_{kj}] = \left[|t_{kj}|^2 \frac{P_{kk}}{P_{jj}} \right] . \tag{8}$$

For lossless systems the reflection and transmission coefficients should sum to unity.

3.1 Reflection at a boundary

Consider an isotropic plate which lies in the region $x \leq 0$ with an edge along the line $x = 0$ as shown in Figure 4. Waves with amplitude $\mathbf{a}^-$ are incident upon the boundary and generate only reflected waves. Any boundary condition in terms of the nodal dofs and nodal forces can be written as $\mathbf{Af} + \mathbf{Bq} = \mathbf{0}$. The dofs and the internal forces can be further projected onto the wave domain using Equation 6, yielding

$$\mathbf{A}(\mathbf{\Phi}_\mathbf{f}^+ \mathbf{a}^+ + \mathbf{\Phi}_\mathbf{f}^- \mathbf{a}^-) + \mathbf{B}(\mathbf{\Phi}_\mathbf{q}^+ \mathbf{a}^+ + \mathbf{\Phi}_\mathbf{q}^- \mathbf{a}^-) = \mathbf{0} . \tag{9}$$

The incident and reflected waves are related by the reflection matrix which follows as

$$\mathbf{r} = -\left[\mathbf{A\Phi}_\mathbf{f}^+ + \mathbf{B\Phi}_\mathbf{q}^+\right]^{-1} \left[\mathbf{A\Phi}_\mathbf{f}^- + \mathbf{B\Phi}_\mathbf{q}^-\right] . \tag{10}$$

3.2 FE/WFE method for a joint of finite dimensions

Analytical results for the scattering coefficients exist for few simple cases, e.g. the reflection coefficients of waves in a simply supported or fixed edge of an isotropic plate. For more complicated structures and joints of finite dimension the hybrid FE/WFE approach is proposed. Details about the FE/WFE approach in case of joined waveguides can be found in [6, 16].

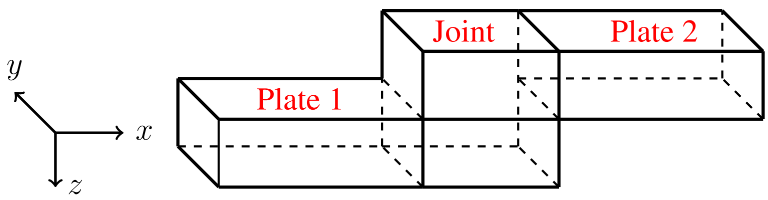

Figure 5: Schematic of two bonded plates. The overlapping region of the two plates is considered the joint.

Consider two plates and a joint as they are illustrated in Figure 5. The FE/WFE approach relies on modelling the plates by using the WFE method, as it was described in section 2, and on modelling the joint by using standard FE methods. A segment of the joint is modelled using standard FE; the stiffness and mass matrices **K** and **M** of a segment of the joint are used to formulate the dynamic stiffness matrix of the joint $\mathbf{D} = \mathbf{K} - \omega^2\mathbf{M}$. In principle, the scattering properties of a joint can be found by applying equations of equilibrium and continuity at the interface nodes between the joints and the plates. For this aim, it is assumed that the interfaces have compatible meshes. The time harmonic behaviour of the joint is described through

$$\mathbf{D}\begin{Bmatrix}\mathbf{Q}_i\\ \mathbf{Q}_n\end{Bmatrix} \equiv \begin{bmatrix}\widetilde{\mathbf{D}}_{ii} & \widetilde{\mathbf{D}}_{in}\\ \widetilde{\mathbf{D}}_{ni} & \widetilde{\mathbf{D}}_{nn}\end{bmatrix}\begin{Bmatrix}\mathbf{Q}_i\\ \mathbf{Q}_n\end{Bmatrix} = \begin{Bmatrix}\mathbf{F}_i\\ \mathbf{F}_n\end{Bmatrix}, \tag{11}$$

where **Q** and **F** are vectors of dofs and of internal nodal forces. Since no external forces are applied at the non-interface nodes, i.e., $\mathbf{F}_n = \mathbf{0}$, then Equation 11 reduces to

$$\mathbf{D}_{ii}\mathbf{Q}_i = \mathbf{F}_i \quad \text{where} \quad \mathbf{D}_{ii} = \widetilde{\mathbf{D}}_{ii} - \widetilde{\mathbf{D}}_{in}\widetilde{\mathbf{D}}_{nn}^{-1}\widetilde{\mathbf{D}}_{ni}, \quad \text{and} \quad \mathbf{Q}_n = -\widetilde{\mathbf{D}}_{nn}^{-1}\widetilde{\mathbf{D}}_{ni}\mathbf{Q}_i\,. \tag{12}$$

By applying the periodicity conditions, the nodal dofs and forces at the interface are expressed in terms of the dofs and forces of the plate. Equation 12 can be expressed in the wave domain and the scattering matrix, which relates the incoming and outgoing waves with $\mathbf{a}^- = \mathbf{s}\mathbf{a}^+$, is finally given by

$$\mathbf{s} = -\left[\mathbf{D}_{ii}\boldsymbol{\Phi}_{\mathbf{q}}^- - \boldsymbol{\Phi}_{\mathbf{f}}^-\right]^{-1}\left[-\boldsymbol{\Phi}_{\mathbf{f}}^+ + \mathbf{D}_{ii}\boldsymbol{\Phi}_{\mathbf{q}}^+\right]. \tag{13}$$

4 NUMERICAL RESULTS

In this section, numerical examples are presented to demonstrate the developed method. The first example is of a plate with a simply supported edge. The next one is about two bonded plates with the same properties and the last one is of two joined laminated plates. In the following, all properties and dimensions are in SI units.

4.1 Isotropic plate with simply supported edge

For the first example a plate in the (x-y) plane with simply supported edge and three dofs has been chosen, see Figure 4. The plate has thickness $h = 3 \times 10^{-3}$ and material properties given by the values $\rho = 2700$, $E = 0.71 \times 10^{11}$ and $\nu = 0.28$. The boundary conditions are: the displacement in the z direction is zero and the bending moment along the x axis is zero. The wavenumbers are analytically known [2, 3] and the numerical computations can validate the WFE model, Figure 6a.

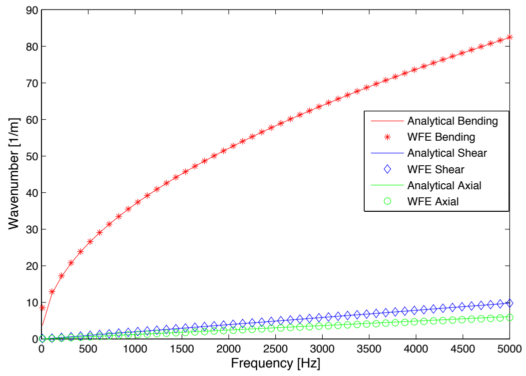

(a) Dispersion curves for the isotropic plate.

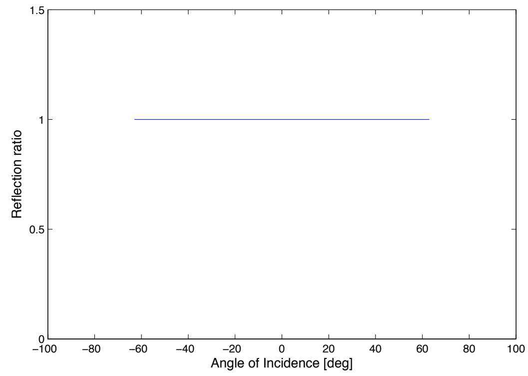

(b) Reflection ratio wrt the angle of incidence.

Figure 6: Isotropic plate with simply supported edge.

Due to the boundary there exist only reflected power and the analytic value of the reflection ratio is equal to one. Computing the reflection matrix in terms of the wavemodes by using Equation 10 the reflection ratio with respect to the angle of incidence is shown in Figure 6b.

4.2 Identical bonded plates

The structure in the second example comprises of two joined identical isotropic plates with the same material properties as in the example of subsection 4.1 and a joint as shown in Figure 5. The hybrid FE/WFE model as described in subsection 3.2 allows the computation of the reflection and transmission coefficients of the joint. For motion along the x-axis, i.e., $\theta = 0°$ and for different frequencies, the power ratio between two bending-type waves is equally distributed between reflection and transmission as shown in Figure 7a.

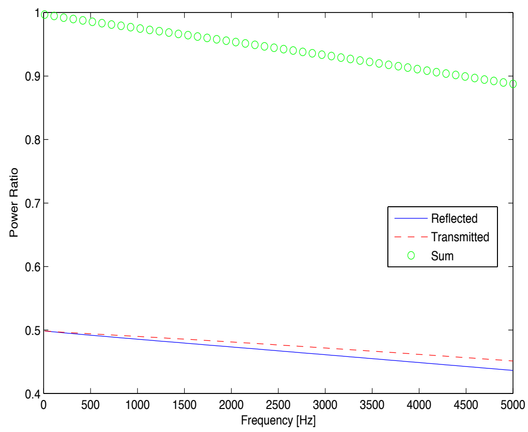

(a) Power reflection and transmission coefficients for propagation angle $\theta = 0°$.

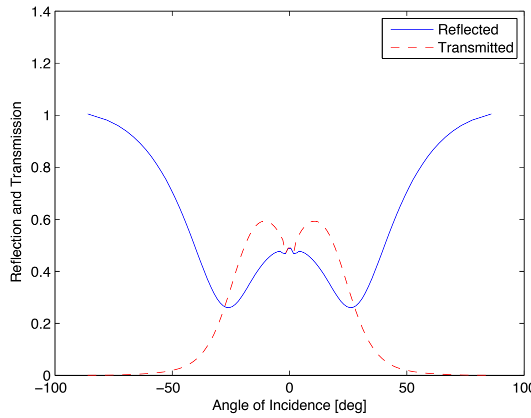

(b) Power reflection and transmission coefficients between two bending-type waves at 1 kHz.

Figure 7: Power reflection and transmission coefficients between two bending-type waves in case of identical bonded isotropic plates.

One can also investigate the influence of the angle of incidence, θ, on the reflection and transmission. Figure 7b shows the power reflection and transmission coefficients for bending-to-bending reflection and transmission at 1 kHz with respect to the incidence angle range $(-90°, 90°)$. For propagation angle $\theta = 0°$ the reflection and transmission ratios are equal (≈ 0.5). While the propagation angle is increasing, the reflection ratio is increasing too. At an incidence angle $\theta \approx 90°$, which corresponds to wave propagation in the y-direction, the reflection ratio is equal to one and the transmission ratio is zero.

4.3 Bonded plates made of composite materials

The plates in the third example are two laminated plates that have the same thickness and properties, and are attached to each other by an adhesive with properties $E = 2.95 \times 10^9$, $\rho = 1100$ and $\nu = 0.286$. Each plate comprises a light, soft foam core sandwiched between two skins. Each skin is made of four layers of graphite epoxy whose material properties along the axes x', y' and z' of orthotropy are $E_{x'} = 144.48 \times 10^9$ and $E_{y'} = E_{z'} = 9.63 \times 10^9$; the shear moduli are $G_{x'y'} = G_{x'z'} = G_{y'z'} = 4.128 \times 10^9$; Poisson's ratios are $\nu_{x'y'} = \nu_{z'y'} = 0.02$ and $\nu_{x'z'} = 0.3$; the density is $\rho = 1389$ and the material loss factor is $\eta = 0.01$.

The layup of the inner (i.e., bottom) skin is $[0/90/90/0]$ degrees and that of the outer (i.e., top) skin is $[90/0/0/90]$ degrees, and each skin is 4×10^{-3} thick (with each laminate being 1mm thick). The core is a polymethacrylamide ROHACELL foam which is isotropic with modulus of elasticity $E = 0.18 \times 10^9$, density $\rho = 1100$ and Poisson's ratio $\nu = 0.286$. For the WFE modelling, SOLID45 elements of ANSYS were meshed through the thickness of each plate.

In Figure 8a the numerically competed values of the wavenumbers of all retained waves are plotted. In this figure one can distinguish the wavenumbers which correspond to the standard waves (i.e., axial, shear and bending). These are also separately shown in Figure 8b. Moreover, there can also be observed and more complicated waves. These are expected to cut-on (i.e. become propagating waves) at higher frequencies as Figure 8a shows. Since there are no known analytical values for these wavenumbers, WFE method is a valuable tool to evaluate the wave characteristics of the plates.

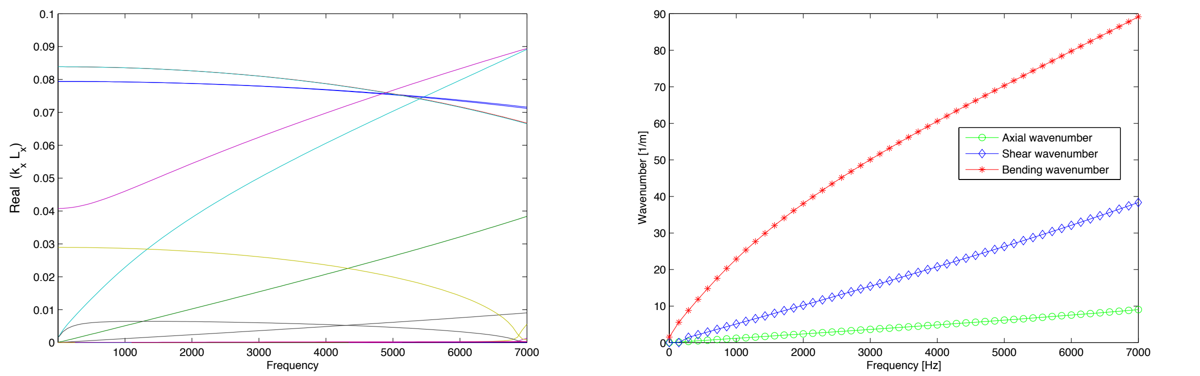

(a) The wavenumbers of all the retained waves after the filtering.

(b) The axial, shear and bending wavenumbers of the waves.

Figure 8: Dispersion curves for the laminated plate in case of propagation angle $\theta = 0$.

Concerning the reflection and transmission coefficients between two bending type waves one can see from Figure 9a that for propagation along the x-axis and lower frequencies, the transmission ratio is higher than the reflection ratio. On the other hand, for higher frequencies there is almost no transmitted power. At low frequencies, the sandwiched behave similar to orthotropic plates with a "near" equi-partition between reflected and transmitted power. As the frequency increases, the role of the joint becomes more apparent and it acts as an impedence which causes the bending waves to reflect into the "source" plate. The discontinuities that are observed above 4.5 kHz can be attributed to wavemode conversions where the waves cannot be purely classified. Similar results are observed for the power ratios at 1kHz for a varying angle of incidence, see Figure 9b. In particular, the transmitted power is decreasing while the angle of propagation is getting bigger and for an angle $\theta > 45°$ there are only reflected waves.

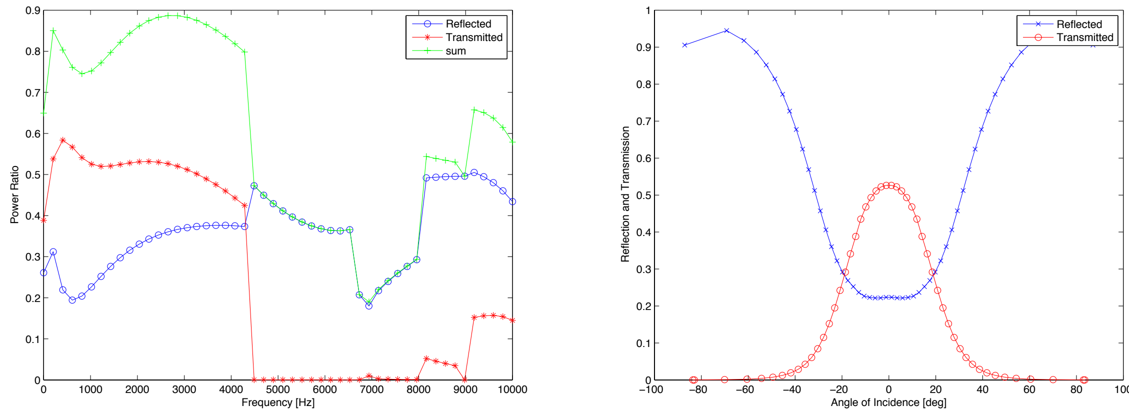

(a) Power reflection and transmission coefficients between two bending-type waves for $\theta = 0°$.

(b) Power reflection and transmission coefficients between two bending-type waves at 1 kHz.

Figure 9: Power reflection and transmission coefficients between two bending-type waves in case of bonded laminates.

5 CONCLUSION

In this paper the WFE method for two dimensional structures has been implemented not only for isotropic plates but also for laminates. The scattering matrix of the joints, when joined plates are considered has also been computed by means of the hybrid FE/WFE approach. Combining the wave characteristics of the plates with the scattering properties of joint, the power reflection and transmission ratios are estimated. The findings of this paper provide valuable knowledge regarding the propagation of waves in the structures under consideration, especially for the cases where analytical results are not known or too difficult to be found.

REFERENCES

[1] J.N. Reddy. *Mechanics of Laminated Composite Plates: Theory and Analysis*. CRC Press, 1996.

[2] K. F. Graff. *Wave Motion in Elastic Solids*. Dover Publications Inc., New York, 1975.

[3] L. Cremer, M. Heckel, and B. A. T. Petersson. *Structure-Borne Sound*. Springer, third edition, 2005.

[4] Y A Abdel-Rahman. *Matrix Analysis of Wave Propagation in Periodic Systems*. PhD thesis, 1979.

[5] B. R. Mace and E. Manconi. Modelling wave propagation in two-dimensional structures using finite element analysis. *Journal of Sound and Vibration*, 318(4-5):884 – 902, 2008.

[6] J. M. Renno and B. R. Mace. Calculating the forced response of two-dimensional homogeneous media using the wave and finite element method. *Journal of Sound and Vibration*, 330(24):5913–5927, 2011.

[7] B. R. Mace, D. Duhamel, M. J. Brennan, and L. Hinke. Finite element prediction of wave motion in structural waveguides. *Journal of the Acoustical Society of America*, 117(5):2835 – 2843, 2005.

[8] M. Maess, N. Wagner, and L. Gaul. Dispersion curves of fluid filled elastic pipes by standard fe models and eigenpath analysis. *Journal of Sound and Vibration*, 296(1-2):264 – 276, 2006.

[9] J.-M. Mencik and M.N. Ichchou. Wave finite elements in guided elastodynamics with internal fluid. *International Journal of Solids and Structures*, 44(7-8):2148 – 2167, 2007.

[10] Elisabetta Manconi and Brian R. Mace. Wave characterization of cylindrical and curved panels using a finite element method. *Journal of the Acoustical Society of America*, 125(1):154 – 163, 2009.

[11] Jamil M. Renno and Brian R. Mace. Calculating the forced response of cylinders and cylindrical shells using the wave and finite element method. *Journal of Sound and Vibration*, 333(21):5340 – 5355, 2014.

[12] D. Duhamel, B. R. Mace, and M. J. Brennan. Finite element analysis of the vibrations of waveguides and periodic structures. *Journal of Sound and Vibration*, 294(1-2):205 – 220, 2006.

[13] R. S. Langley and K. Heron. Elastic wave transmission through plate/beam junctions. *Journal of Sound and Vibration*, 143:241–253, 1990.

[14] I. Bosmans and T. Nightingale. Modeling vibrational energy transmission at bolted junctions between a plate and a stiffening rib. *Journal of Acoustical Society of America*, 109(3):999–1010, 2001.

[15] S.J. Walsh and R.G. White. Vibrational power transmission in curved beams. *Journal of Sound and Vibration*, 233(3):455 – 488, 2000.

[16] J. M. Renno and B. R. Mace. Calculation of reflection and transmission coefficients of joints using a hybrid finite element/wave and finite element approach. *Journal of Sound and Vibration*, 332(9):2149–2164, April 2013.

[17] W.X. Zhong and F.W. Williams. On the direct solution of wave propagation for repetitive structures. *Journal of Sound and Vibration*, 181(3):485 – 485, 1995.

[18] W.X. Zhong, F.W. Williams, and A. Y. T. Leung. Symplectic analysis for periodical electro-magnetic waveguides. *Journal of Sound and Vibration*, 267(2):227 – 244, 2003.

[19] Y. Waki, B. R. Mace, and M. J. Brennan. Numerical issues concerning the wave and finite element method for free and forced vibrations of waveguides. *Journal of Sound and Vibration*, 327(1-2):92–108, 2009.